Fermi National Accelerator Laboratory

TM-1571

Understanding and Improving the Fermilab Booster High Field Orbit

Y. Chao, L. Ketcham, and C. D. Moore
Fermi National Accelerator Laboratory
P.O. Box 500, Batavia, Illinois

March 1989

Operated by Universities Research Association, Inc., under contract with the United States Department of Energy

1. Introduction

This note is an account of the authors' effort in both understanding the Booster high field orbit and controlling it through displacements of the main combined function magnets. We were able to achieve the second goal with considerable accuracy while having limited success with the first, due to insufficient knowledge of the Booster dynamics. This work was initiated in Spring 1987 with the orbit control via magnet moves the chief purpose. A series of magnet moves in 1987 and 1988 resulting from this study testified to its reliability. The understanding of the Booster orbit in general remains an ongoing process in which we keep modifying our model with the hope of eventually having a quantitative grasp of the closed orbit and being able to manipulate it with more flexibility and accuracy.

In section 2 we give a brief description of the Booster environment in which the magnet moves are carried out, together with background information concerning the magnet moves. The method we use is discussed in section 3. The result of the moves is documented in section 4. In section 5 our effort to understand the Booster high field orbit is given a detailed account.

2. The Booster and other background information

Fermilab Booster is an alternating gradient proton synchrotron with an extraction kinetic energy of 8 GeV. Bending and focusing of the beam are done through the 96 combined function magnets grouped into 24 identical DOFOFODO periods. Table 1 lists the relevant parameters of the Booster. The low field orbit (up to ~ 2 GeV/C in momentum) can be effectively controlled by the correction dipole packages installed around the ring. Near extraction energy, the correction dipoles are essentially of no consequence. It was observed before this work started that the horizontal high field orbit underwent an abnormally big excursion inward near short section 10 (see Figure 1). Radiation survey supported this observation. The first incentive of this work is therefore to correct this orbit excursion with the minimal disturbance on the Booster hardware and, if possible, to modify the high field orbit towards a smoother one.[1]

In principle the major sources of high field orbit distortion for a fixed energy are the transverse displacement of the main (quadrupole) magnet center from the design orbit, to be called the **offset** in the following, and the rotation around the beam axis of the main (dipole) magnet with respect to the nominal orientation, to be called the **roll** in the following. In the Booster the main dipole and quadrupole magnets are integrated into one piece as combined function magnets. A constantly updated survey record by the Fermilab survey staff keeps track of the offsets and

[1] To determine which part of the orbit we want to fix, we simply look at the display of the BPM readings and try to eliminate the outstanding peaks. The console program "Cusp out the Booster" was also employed as a consulting device.

rolls of all 96 of these magnets due to alignment errors or deterioration with time. The corrections to the survey marks used in such survey procedures are kept in a public VAX file: FNAL::USR$ROOT29:[ALIGNMENT.BOOSTER]BOUTPUT.DAT. Figures 2(a) and 2(b) show the horizontal and vertical offsets of these magnets as of April 1987 before any changes were made. Figure 3 shows the roll values of same. We noticed that a set of deliberate moves existed when the Booster was first put into operation in order to exploit the good field region of the magnets. The D-magnets were moved inward by 0.053 inches and the F-magnets outward by 0.040 inches. The effects of these moves were obviously taken into account in determining the main bending field and ideal orbit position, since otherwise the overall effect of these moves on the horizontal orbit would have been as shown in Figure 2(c), an overall outward displacement of the order of 10 mm at all times in the cycle. The solid line in Figure 2(a) shows the offsets with these deliberate moves taken out, while the dotted lines and circles are the actual survey data showing a zigzaging about the solid line due to these deliberate moves. It is clear that the solid line is more of a measure of how far the current situation has deteriorated from the original desired situation. Our work concerning the magnet moves is based on the solid line, namely ignoring the deliberate moves, since it is the difference in the orbits alone that interests us, and also because it is the magnet position after the deliberate moves that we want to restore to, not the one before. Table 2 lists all the numerical values.

The data in figure 2(a) were obtained by fitting the raw measurement to a theoretical model of the Booster geometry. This is explained in detail in Appendix A. Our experience of magnet moves shows that for practical purposes these data are sufficient for explaining the behavior of the orbit.

Besides affecting the vertical closed orbit, the rolls in the main magnet also contribute to the linear coupling. An independent study (Fermilab exp. note 159) of the Booster beam dynamics shows that the amount of linear coupling agrees very well with that predicted by the roll data alone.

3. Method and criteria used in determining the moves

(a). Evaluating the closed orbit as a function of field defects

A computer program was developed using the Booster lattice to calculate its closed orbit with the input of main magnet offsets, rolls, and correction dipole settings. It is constructed in the following way:

The closed orbit of the beam with respect to the design orbit can be broken down into two parts: the betatron oscillation part due to the focusing forces and the "cusps" due to local dipole field defects. Offsets and rolls, which translate into kicks inside the magnets, go under the second category. In obtaining the closed orbit, we have to find both the one turn matrix corresponding to the betatron oscillation part and the total effect from all the dipole field imperfections.

In each plane the vector (x,p), or position and slope, is subjected to the action of matrices corresponding to all nominal optical elements around the Booster. The transfer matrices of the main magnets are based on the Booster parameters given in TM-405. To account for the finite extent of the main magnets, the effect of focusing has been divided into 4 equal parts over the length of the magnet. The **one-turn matrix M**, or the matrix product of all the constituent matrices (without offsets, rolls, or correction dipoles) once around the Booster, is obtained simply by assigning (1,0) and (0,1) to (x,p) respectively and looking at the resulting vectors after one turn. We then apply the same matrices, together with all field imperfections, on the vector (0,0), which gives us the part of the first turn orbit due to all field imperfections when the beam is injected with no injection error. This gives us a vector (x',p') at the end of one turn. In the last step all offsets and rolls of the main magnets are again divided into 4 equal parts over the length of the magnet. The closed orbit (x_{co},p_{co}) at the starting point is then given by

$$(x_{co},p_{co}) = (1\text{-}M)^{-1}\bullet(x',p')$$

where matrix multiplication is implied on the right hand side. The vector (x_{co},p_{co}) is then subjected to the same matrices and kicks due to imperfections all around the ring to give the closed orbit at every BPM location.

This program is used as a consulting device to give us instant prediction as to how the orbit will change for a given change in the offsets, the rolls, the dipole settings, or combinations thereof. Such combinations in turn result from experimenting with many different scenarios under constraints mentioned later in this note. The orbit change induced by the magnet moves is in general not localized. Thus usually after the locations of a particular set of moves are determined, the work is reduced to an optimization process in which we try to minimize the orbit excursion at as many places as possible while keeping everything else within reasonable limits.

(b). Additional considerations

For any desired change in the global closed orbit, we can usually find more than one moving scenario which would do the job. Other criteria have to be used to single out the best option. These can be enumerated as follows:

1. The least total number of moves
2. The moves with the smallest magnitudes
3. Moves away from injection and extraction areas
4. Moves acting to reduce the specific offsets of the magnets in question
5. Moves acting to reduce the tension induced on the beam pipe between magnets caused by initial offsets or previous moves.

With these criteria coming into the game, our choice is greatly limited and as can be seen from the last point, it will become more and more stringent as we perform more and more moves. We managed to plan all of our moves so far (6 horizontal and 5 vertical in two moving plans one year apart) so that none of the above criteria was violated. Further moves would certainly demand more caution.

(c). Special moving combinations

From the constraint 1 in (b), it is best to correct the orbit with the least number of moves. It turns out to be possible to use the so called **2-bumps**, consisting of two moves $N \cdot \pi$ apart in betatron phase, to induce an orbit change spanning several periods of the Booster and correcting the orbit at many locations at the same time. The only condition for the use of the 2-bumps is that the separation of $N \cdot \pi$ has to be reasonably accurate. The lattice parameters (β and betatron phase ϕ) at the locations of all main magnets are given in Table 3. Our selection of the 2-bumps was based on this table. Figure 4 demonstrates the effect of a 2-bump with two moves $3 \cdot \pi$ apart. The general case is self-evident. This technique was employed in the March 1988 move to correct the orbit across 11 periods, or almost half way around the ring, with only 2 moves. It proved to be quite successful.

To correct very localized orbit excursions the local 3-bumps are used. These are moves in 3 consecutive main magnets so that only the orbit at one straight section is significantly affected. We worked out the moving ratios required of such combinations in order to change the local orbit at a given long or short straight section. These are given in Table 4.

In reality we seldom encountered the need of a very localized move since the high field closed orbit displays a characteristic length consistent with the betatron wavelength which spans several periods. The most favorite approach adopted is to first try to fix the orbit at as many points as possible through a 2-bump, even if the overall effect is not quite localized. We then try to find a strategic moving point in the ring (there can be more than one) by phase counting or simply trial and error to neutralize the nonlocal effect. Of course all this is still subject to the constraints 3,4,and 5 in (b), which complicated the picture considerably.

4. The result

Table 5 lists all the magnet moves made after May 1987. One vertical move in March 1988 suffered from a mistake in the use of the survey apparatus, which was later corrected. Figures 5 and 6 show the calculated and actual change of the orbit by the magnet moves. Details are given in individual captions of the plots. The actual outcome of the moves matched the calculation to a very high degree of accuracy both in the global pattern and in the specific magnitudes. For example, it was predicted that the horizontal orbit change in the two crucial points, L10 and S10, would be 2.9 mm and 6.9 mm respectively. The actual changes were 2.8 mm and 6.5 mm. The prediction gave a very localized pattern in the orbit change, which was also observed. It should also be pointed out that the BPM readings at horizontal S1 and L20 were behaving erratically during March 1988 and also the vertical position of the L2 BPM was moved during the shutdown. These BPM readings, and the discrepancy between the predicted and observed orbit changes at

these locations, should therefore be viewed with skepticism.

Figures 7(a) and (b) show the impact of the moves made on the original offsets of Figures 2(a) and (b). Their significance was mentioned in criteria 4 and 5 in section 3(b). We are largely able to conform to these criteria.

5. Predicting the global high field orbit

Considerable effort has been devoted to understanding the high field orbit. The purpose is to reconcile the measurements taken independent of the beam and the directly measured beam position itself. The former includes the lattice parameters, the magnet survey data, the correction element settings, the radial feedback effects etc.. It is clear that such an understanding would help us control the Booster orbit much more accurately and reliably. Also in the process of achieving this goal we may discover other parameters relevant to our prediction, or maybe the very method we use would be subject to modification. It is in this sense that this last effort is an ongoing process with improvements added constantly, eventually limited by the hardware accuracy. In the following we report the result we have currently obtained in both planes.

(a) Horizontal

Figure 8 shows the comparison between the horizontal orbit predicted by our model using the main magnet offsets and correction dipole settings and the observed orbit. Both are obtained at t=32.6 msec in the cycle. The predicted orbit is obtained by including the survey data of all 96 magnet offset values in the calculation described in section 3 (a). A complication arises due to the RF radial position feedback loop (**ROFF** loop), which forces the orbit at a pickup point in L18 to be a pre-programmed value. Since this pickup is really 5.07 meters upstream of the L18 BPM (see Figure 9), some interpolation is needed to obtain the beam position at the ROFF pickup in both the predicted and the measured orbits. The difference between these two values is then translated into the additional orbit change caused by the change in momentum offset imposed by the ROFF loop. The interpolation to the beam position at the ROFF pickup is done as follows: The beam positions at S17 and L18 (or L18 and S18) are given by the orbit calculation. These numbers are however insufficient for determining the slopes at these 2 locations. This is because the extra kicks between say, S17 and L18 due to the magnet offsets at 17-3, 17-4, and correction dipole in S17 cause the closed orbit to deviate significantly from a simple betatron oscillation. We therefore used a root finding algorithm incorporating all these kicks to solve for the correct slopes at S17 and L18, which give the correct positions at S17 and L18 when all intervening kicks are included. We then use the slope at L18 to extrapolate back to the ROFF pickup point to determine the orbit there.

Figure 8 shows that our prediction basically has the correct phase information reflected in the measured orbit. The mismatch in amplitudes has initiated searches

in various directions without conclusive result. One possibility is that there is a set of unaccounted 2-bump type kicks somewhere between sections 4 and 14. We are not able to confirm this[2]. Our success in predicting the localized orbit amplitudes in magnet moves rules out the likelihood of a drastically wrong model which yields disproportionate magnitudes in the prediction of localized orbit distortion. However it is possible that in going from local to global predictions, small discrepancies add up coherently to give a much enhanced effect. It is currently not clear to us how this can happen though.

(b) Vertical

Besides the main magnet offsets, the magnet rolls come into play as well when we deal with the vertical orbit. This adds to the complexity of the problem. Figure 10 shows the comparison between the predicted and the measured vertical closed orbits taken at t=33.0 msec. We are largely able to explain the observation with our model except near L11, where a large discrepancy is observed. The BPM at L11 has been rechecked and no malfunction was detected. Apart from the unrealistic amplitude, the deviation displays a valid betatron half period covering about 1.13π of the vertical betatron phase, again suggesting a possibly unaccounted 2-bump in the vicinity. This is subject to further investigation.

A need for modifying our model was discovered in the process. This comes out of the fact that in our perturbative treatment of the orbit distortion as described in section 3(a), we intrinsically adopted the absolute horizontal plane used by the surveyors as the plane which the unperturbed orbit sits in. In reality the beam can nonetheless settle into a different "unperturbed" plane which is tilted with respect to our chosen plane. In exact solution of the problem this difference is immaterial. But in perturbative calculations this difference is interpreted as perturbations and its net effect can be large. We modified our approach such that a least square fit routine is used first on the vertical offset data to determine the natural unperturbed plane preferred by the beam. We then recalculate the offsets and rolls with respect to this new plane before we embark on our usual orbit analysis. In the problems we are currently dealing with, the effect due to such consideration is visible but quite small. More detail is provided in Appendix B.

2The program "cusp out the Booster" was used to search for possible large kicks which will account for the discrepancy. We were unable to find a small number of such kicks which satisfy this purpose.

Conclusion

The effort devoted in understanding and improving the Booster closed orbit has been presented in this note. We have achieved considerable success in moving individual magnets (instead of the girder which supports 2 magnets) to correct the high field orbit. This practice also helped to bring some of the magnets back in line with the majority according to the survey data. The well defined procedure can be applied to future moves, although the criteria will be more stringent with more moves.

Our current understanding of the global high field orbit based on the survey offsets gives us a generally correct picture. Room for refinements definitely exists. This will depend on more accurate input of the field survey and magnet measurement. Further improvements in both the survey technique and analysis tools are expected in this ongoing process.

Appendix A. Procedure for determining the horizontal offsets

The question of determining the absolute horizontal beam trajectory of a circular machine is not a trivial one. This is due to the difficulty in coordinating the measurements on widely different objects such as the magnetic field, the effective magnetic length, and the positions of all relevant elements. The cross-influence between the two planes adds to the complexity. These factors are further obscured by the flexibility demanded by beam control such as low energy guide field and radial feedback loops. This ambiguity is then propagated to the alignment errors which are measured against the "ideal" beam trajectory. All these do not cause serious problem when only localized orbit distortion is at issue. But in considering the global behavior of the orbit, this can lead to complication as we have seen in section 5.

The offsets as shown in Table 2 are obtained in 3 steps. First a field survey determines the relative horizontal positions of the elements, then a theoretical model of the Booster beam trajectory was developed using the measured magnet data, finally these two sets of information are reconciled with each other and the resulting discrepancy is interpreted as the offsets, or alignment errors. In the following each of these 3 steps are described.

(a) The field survey

(1). A series of reference monuments within the Booster tunnel were first surveyed to determine their relative positions. There is one such monument for each cell, near the bend center. A control network is established as all 24 such monuments are surveyed and the closing error distributed using the Compass Rule adjustment.

(2). The positions of bushings mounted on top of each magnet near the 2 outer corners relative to the control network as described in (1) are measured. These relative positions will be used later to establish the position of the magnet centers relative to the control network.

(b) The theoretical model

(1). The integrated bend strength and effective field length was used to determine the bend radius of each magnet. The condition that each cell should bend 15 degrees is also checked and satisfied.

(2). The above data and the radial distance from the center to the long straight sections are used in a fitting procedure to determine the overall geometry of the orbit.

(3). The geometry of a single magnet is employed to determine the absolute locations of the bushings according to this theoretical model.

(c) The offsets

(1). Its measured and theoretical locations compared, each bushing on the outer

corners of the magnets is assigned two errors, one radial and one azimuthal. The modeled theoretical orbit is then allowed to rotate about the center rigidly to reduce the overall azimuthal errors in a least square manner. The outcome of this fitting determines the orientation of the theoretical ring and orbit.

(2). The geometry of individual magnets is used to interpolate the offset of the magnet center line from the ideal one, using the offset of the bushings. These are the values presented in table 2.

Appendix B. Effect of a "tilted" orbit plane

It is clear that our method for obtaining the predicted orbit distortion, as described in section 3(a), is perturbative in nature. It is therefore important to know on what unperturbed solution (or ideal orbit) the perturbation correction is built. Different choices of the unperturbed solution can lead to very different results in the perturbation calculation, although it would not have mattered in an exact solution. Such a subtlety was encountered in our prediction of the vertical orbit. The survey data were taken assuming the gravitationally horizontal plane to be the ideal orbit plane. There is no justification a priori for choosing this as the natural ideal orbit plane, though. Figure 11 shows a hypothetical case in which the whole Booster ring plane is rotated by an angle θ about a line passing through the center. The ideal closed orbit in the exact solution should be a circle lying within the tilted plane, with BPM's registering no orbit distortions (of course we assume the BPM's are displaced with the tilted plane). But in a perturbation calculation assuming the ideal orbit to be lying inside the gravitationally horizontal plane, the vertical distance between the two planes will be interpreted as perturbations in terms of magnet offsets and rolls and its effect nonzero, which is not real. In our prediction of the vertical closed orbit, we therefore should be careful enough to filter out such an artifact.

We can work out such artificial offset and roll in the situation of Figure 11. The net effect is such that if the tilt angle is θ and the point of maximum vertical displacement in the ring is denoted P, then the vertical displacement of a point A in the ring which is azimuthally an angle ϕ away from P is

$$D_a = R \cdot \sin(\tan^{-1}(\cos\phi \cdot \tan\theta))$$

where R is the radius, and the corresponding roll is

$$\alpha_a = \tan^{-1}(\cos\phi \cdot \tan\theta)$$

The effect on the offset, roll, and closed orbit as calculated by our perturbation method for θ=0.1 mrad is given in Figure 12. Notice that the effect of such a tilted plane is exactly reproduce by our perturbation calculation based on magnetic kicks. This can serve as an independent check for the validity of our calculation.

We did a least square fit of the measured offsets to a tilted plane by varying the variables θ and ϕ, the azimuthal angle between the point P and center of magnet 24-4. The fitted parameters are

θ = 1.141E-05 rad and ϕ = 2.858 rad

The net contribution of such an offset and roll distribution turns out to be small (at most 0.75 mm) in our case. In principle if a reliable set of absolute BPM measurements exists, then one doesn't need to worry about such artifacts. One however does have to worry in cases where the artificial offset is so large that it renders the linear approximation questionable.

Injection Energy (Kinetic)	204 MeV
Extraction Energy (Kinetic)	8 GeV
Circumference	474.20 meters
Cycle Rate	15 Hz
Number of Bunches	84
RF harmonic number	84
ν_x	6.7
ν_y	6.8
γ_t	5.4
RF frequency(Inj.)	30.31 MHz
RF frequency(Ext.)	52.81 MHz

$$P = A - B\cos G(T - H)$$

where
P is the momentum in GeV/C
T is the time in cycle in ms
$A = 4.76945$ GeV/C
$B = 4.11945$ GeV/C
$G = 0.0942478$
$H = 2.0$ ms

Table 1: Booster parameters

TABLE 2. OFFSETS AND ROLLS FROM THE ORIGINAL SURVEY

(A) THE HORIZONTAL MAGNET OFFSETS (INCHES) AS OF APR. 1987 (BEFORE MOVE)

	D-MAGNET	F-MAGNET	F-MAGNET	D-MAGNET
1	0.208000	0.238000	0.164000	0.040000
2	-0.018000	0.065000	0.077000	-0.016000
3	-0.083000	0.008000	0.022000	-0.058000
4	-0.141000	0.006000	0.061000	-0.037000
5	-0.008000	0.056000	0.054000	-0.050000
6	-0.135000	-0.049000	-0.062000	-0.161000
7	-0.147000	-0.018000	0.008000	-0.117000
8	-0.124000	-0.030000	-0.040000	-0.160000
9	-0.156000	-0.034000	-0.086000	-0.326000
10	-0.077000	0.036000	0.077000	-0.038000
11	0.080000	0.170000	0.098000	0.012000
12	-0.026000	0.144000	0.159000	0.020000
13	0.140000	0.218000	0.207000	0.069000
14	0.111000	0.208000	0.155000	0.019000
15	0.020000	0.058000	0.041000	-0.111000
16	-0.107000	-0.011000	-0.025000	-0.149000
17	-0.142000	-0.027000	-0.032000	-0.133000
18	-0.122000	-0.045000	-0.099000	-0.239000
19	-0.164000	-0.049000	-0.057000	-0.149000
20	-0.127000	-0.017000	0.016000	-0.071000
21	-0.079000	0.012000	0.043000	-0.037000
22	0.009000	0.081000	0.097000	-0.052000
23	-0.002000	0.049000	0.051000	-0.042000
24	0.084000	0.155000	0.177000	-0.106000

MAX. OFFSET= 0.3260 AVE. OFFSET= -0.0059
RMS. OFFSET= 0.1077 AVE. SEPARATION= 0.0788

(B) THE VERTICAL MAGNET OFFSETS (INCHES) AS OF APR. 1987 (BEFORE MOVE)

	D-MAGNET	F-MAGNET	F-MAGNET	D-MAGNET
1	-0.022200	0.016800	0.044800	0.062800
2	0.051800	0.048800	0.040800	0.036800
3	-0.008200	-0.021200	-0.036200	-0.034200
4	0.041800	0.087800	0.136800	0.159800
5	-0.022200	-0.093200	-0.115200	-0.093200
6	-0.020200	-0.004200	0.016800	0.045800
7	-0.078200	-0.053200	-0.074200	-0.017200
8	-0.015200	0.005800	0.004800	0.068800
9	-0.010200	0.004800	-0.005200	0.000800
10	0.070800	0.064800	0.021800	-0.025200
11	0.055800	0.024800	0.019800	0.066800
12	0.063800	0.118800	0.119800	0.108800
13	0.076800	0.077800	0.026800	0.030800
14	0.046800	-0.010200	-0.053200	-0.047200
15	-0.001200	-0.004200	-0.013200	0.005800
16	0.027800	0.047800	0.039800	0.044800
17	-0.001200	-0.006200	0.000800	0.018800
18	0.008800	0.027800	0.019800	0.006800
19	-0.005200	-0.021200	-0.026200	-0.014200
20	0.000800	-0.005200	-0.009200	-0.007200
21	-0.020200	-0.006200	-0.004200	0.001800
22	-0.165200	-0.089200	-0.101200	-0.107200
23	-0.122200	-0.103200	-0.091200	-0.104200
24	-0.098700	-0.071200	-0.057200	-0.005200

MAX. OFFSET= 0.1652 AVE. OFFSET= 0.0000
RMS. OFFSET= 0.0595 AVE. SEPARATION= 0.0277

(C) THE MAGNET ROLLS (MILIRADIANS) AS OF APR. 1987 (BEFORE MOVE)

	D-MAGNET	F-MAGNET	F-MAGNET	D-MAGNET
1	0.603000	0.905000	0.905000	0.938000
2	1.014000	1.349000	2.220000	0.243000
3	1.609000	0.469000	0.268000	1.441000
4	1.273000	1.642000	1.215000	0.318000
5	0.302000	0.268000	1.098000	0.545000
6	0.318000	0.084000	1.131000	0.042000
7	0.402000	0.117000	0.293000	-1.433000
8	1.098000	1.475000	0.922000	2.421000
9	0.536000	0.151000	1.106000	1.165000
10	1.257000	0.570000	0.721000	0.653000
11	-1.089000	1.592000	2.145000	0.335000
12	2.220000	0.821000	1.885000	0.411000
13	0.000000	0.000000	0.419000	0.503000
14	-0.084000	0.385000	0.251000	1.542000
15	1.475000	0.385000	0.603000	0.788000
16	1.408000	0.989000	1.793000	0.838000
17	0.369000	0.838000	0.905000	0.519000
18	0.637000	0.620000	0.788000	0.620000
19	0.000000	-0.335000	0.603000	-0.570000
20	0.553000	0.369000	0.653000	0.285000
21	0.436000	0.067000	0.687000	0.302000
22	0.000000	0.151000	0.905000	0.034000
23	-0.704000	-2.027000	-0.335000	-0.335000
24	-1.692000	-0.235000	0.285000	0.687000

TABLE 3 LATTICE FUNCTIONS AVERAGED OVER EACH MAGNET FROM END OF LS1
(PHI in RADIAN, BETA in METER)

# 1	H-PHI	V-PHI	H-BET	V-BET	# 9	H-PHI	V-PHI	H-BET	V-BET	# 17	H-PHI	V-PHI	H-BET	V-BET
D	0.190	0.097	12.399	16.930	D	14.222	14.339	12.399	16.930	D	28.254	28.580	12.399	16.930
F	0.369	0.447	30.661	6.541	F	14.401	14.689	30.661	6.541	F	28.433	28.931	30.661	6.541
F	0.498	1.141	27.463	7.911	F	14.530	15.383	27.463	7.911	F	28.562	29.625	27.463	7.911
D	0.722	1.427	9.971	18.795	D	14.754	15.669	9.971	18.795	D	28.785	29.911	9.971	18.795
# 2	H-PHI	V-PHI	H-BET	V-BET	# 10	H-PHI	V-PHI	H-BET	V-BET	# 18	H-PHI	V-PHI	H-BET	V-BET
D	1.944	1.877	12.399	16.930	D	15.976	16.119	12.399	16.930	D	30.008	30.361	12.399	16.930
F	2.123	2.227	30.661	6.541	F	16.155	16.469	30.661	6.541	F	30.187	30.711	30.661	6.541
F	2.252	2.921	27.463	7.911	F	16.284	17.163	27.463	7.911	F	30.316	31.405	27.463	7.911
D	2.476	3.207	9.971	18.795	D	16.508	17.449	9.971	18.795	D	30.539	31.691	9.971	18.795
# 3	H-PHI	V-PHI	H-BET	V-BET	# 11	H-PHI	V-PHI	H-BET	V-BET	# 19	H-PHI	V-PHI	H-BET	V-BET
D	3.698	3.657	12.399	16.930	D	17.730	17.899	12.399	16.930	D	31.762	32.141	12.399	16.930
F	3.877	4.007	30.661	6.541	F	17.909	18.249	30.661	6.541	F	31.941	32.491	30.661	6.541
F	4.006	4.702	27.463	7.911	F	18.038	18.944	27.463	7.911	F	32.070	33.186	27.463	7.911
D	4.230	4.987	9.971	18.795	D	18.262	19.229	9.971	18.795	D	32.293	33.471	9.971	18.795
# 4	H-PHI	V-PHI	H-BET	V-BET	# 12	H-PHI	V-PHI	H-BET	V-BET	# 20	H-PHI	V-PHI	H-BET	V-BET
D	5.452	5.437	12.399	16.930	D	19.484	19.679	12.399	16.930	D	33.516	33.921	12.399	16.930
F	5.631	5.787	30.661	6.541	F	19.663	20.029	30.661	6.541	F	33.695	34.271	30.661	6.541
F	5.760	6.482	27.463	7.911	F	19.792	20.724	27.463	7.911	F	33.824	34.966	27.463	7.911
D	5.984	6.768	9.971	18.795	D	20.016	21.010	9.971	18.795	D	34.047	35.251	9.971	18.795
# 5	H-PHI	V-PHI	H-BET	V-BET	# 13	H-PHI	V-PHI	H-BET	V-BET	# 21	H-PHI	V-PHI	H-BET	V-BET
D	7.206	7.218	12.399	16.930	D	21.238	21.459	12.399	16.930	D	35.270	35.701	12.399	16.930
F	7.385	7.568	30.661	6.541	F	21.417	21.810	30.661	6.541	F	35.449	36.052	30.661	6.541
F	7.514	8.262	27.463	7.911	F	21.546	22.504	27.463	7.911	F	35.578	36.746	27.463	7.911
D	7.738	8.548	9.971	18.795	D	21.770	22.790	9.971	18.795	D	35.801	37.032	9.971	18.795
# 6	H-PHI	V-PHI	H-BET	V-BET	# 14	H-PHI	V-PHI	H-BET	V-BET	# 22	H-PHI	V-PHI	H-BET	V-BET
D	8.960	8.998	12.399	16.930	D	22.992	23.240	12.399	16.930	D	37.024	37.482	12.399	16.930
F	9.139	9.348	30.661	6.541	F	23.171	23.590	30.661	6.541	F	37.203	37.832	30.661	6.541
F	9.268	10.042	27.463	7.911	F	23.300	24.284	27.463	7.911	F	37.332	38.526	27.463	7.911
D	9.492	10.328	9.971	18.795	D	23.524	24.570	9.971	18.795	D	37.555	38.812	9.971	18.795
# 7	H-PHI	V-PHI	H-BET	V-BET	# 15	H-PHI	V-PHI	H-BET	V-BET	# 23	H-PHI	V-PHI	H-BET	V-BET
D	10.714	10.778	12.399	16.930	D	24.746	25.020	12.399	16.930	D	38.778	39.262	12.399	16.930
F	10.893	11.128	30.661	6.541	F	24.925	25.370	30.661	6.541	F	38.957	39.612	30.661	6.541
F	11.022	11.823	27.463	7.911	F	25.054	26.065	27.463	7.911	F	39.086	40.306	27.463	7.911
D	11.246	12.108	9.971	18.795	D	25.278	26.350	9.971	18.795	D	39.309	40.592	9.971	18.795
# 8	H-PHI	V-PHI	H-BET	V-BET	# 16	H-PHI	V-PHI	H-BET	V-BET	# 24	H-PHI	V-PHI	H-BET	V-BET
D	12.468	12.558	12.399	16.930	D	26.500	26.800	12.399	16.930	D	40.532	41.042	12.399	16.930
F	12.647	12.908	30.661	6.541	F	26.679	27.150	30.661	6.541	F	40.711	41.392	30.661	6.541
F	12.776	13.603	27.463	7.911	F	26.808	27.845	27.463	7.911	F	40.840	42.087	27.463	7.911
D	13.000	13.889	9.971	18.795	D	27.031	28.130	9.971	18.795	D	41.063	42.372	9.971	18.795

TABLE 4 Ratios of 2-bumps and 3-bumps used in the magnet moves

(A) 2-bumps:

Magnet moves:

1-1	(D)	up	0.01409 inches
4-3	(F)	up	0.01485 inches

Effect:

Orbit at L2: +1 mm
Orbit at L4: -1 mm

(B) 3-bumps:

In the following Ln and Sn denote the nth long and short sections respectively

3-bumps to change orbit at Ln (n not equal 1) by +1 mm:

Magnet moves:

(n-1)-4	(D)	up	0.03832 inches
n-1	(D)	down	0.08522 inches
n-2	(F)	down	0.08835 inches

3-bumps to change orbit at L1 by +1 mm:

Magnet moves:

24-3	(F)	down	0.08941 inches
24-4	(D)	down	0.08349 inches
1-1	(D)	up	0.03627 inches

3-bumps to change orbit at Sn by +1 mm:

Magnet moves:

n-1	(D)	up	0.12297 inches
n-2	(F)	up	0.27884 inches
n-3	(F)	down	0.09780 inches

TABLE 5 History of magnet moves in Fermilab Booster since May 1987:

May 1987 :

Horz. :	9-3	(F)	0.0560"	out
	11-1	(D)	0.0800"	in
Vert. :	22-1	(D)	0.0580"	up
	24-1	(D)	0.0455"	up
	5-2	(F)	0.0520"	up

March 1988 :

Horz. :	7-4	(D)	0.070"	out
	18-2	(F)	0.050"	out
	20-3	(F)	0.025"	out
	22-1	(D)	0.055"	in
Vert. :	2-2	(F)	0.030"	down (actually 0.060" down)
	5-3	(F)	0.030"	up

May 1988 :

Vert. :	2-2	(F)	0.030"	up

(MM) 05/17/87 1239

SNAPSHOT FRAME .0343
FILE 115 05/16/87 1128:50 17
MORE HI FIELD ORBIT W/NEW ROFF

L1	5.15	L7	-1.85	L13	1.93	L19	.630
S1	-4.40	S7	-9.35	S13	-.41	S19	.410
L2	.610	L8	3.69	L14	-.511	L20	4.37
S2	-7.29	S8	3.53	S14	-7.28	S20	-3.27
L3	2.73	L9	3.61	L15	2.78	L21	-5.91
S3	-6.01	S9	-4.11	S15	1.83	S21	-10.2
L4	-.860	L10	-2.81	L16	2.93	L22	-4.07
S4	-8.73	S10	-16.9	S16	-2.13	S22	-9.55
L5	1.66	L11	-3.81	L17	-2.19	L23	1.41
S5	-.360	S11	-6.99	S17	-11.6	S23	2.95
L6	1.53	L12	5.32	L18	-2.06	L24	.13
S6	-7.68	S12	-.210	S18	-10	S24	-5.70

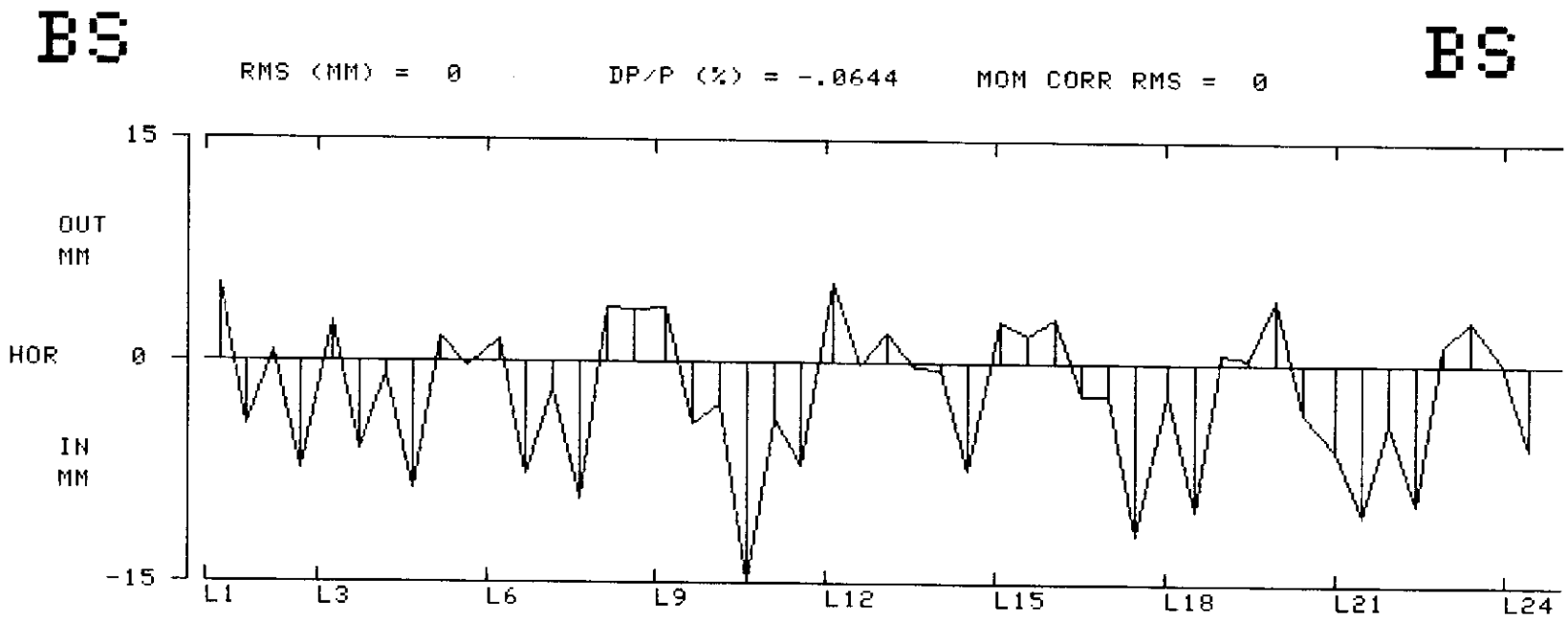

Figure 1 Booster high field horizontal orbit before magnet moves

Figure 2(a): Horizontal magnet offset 04/87

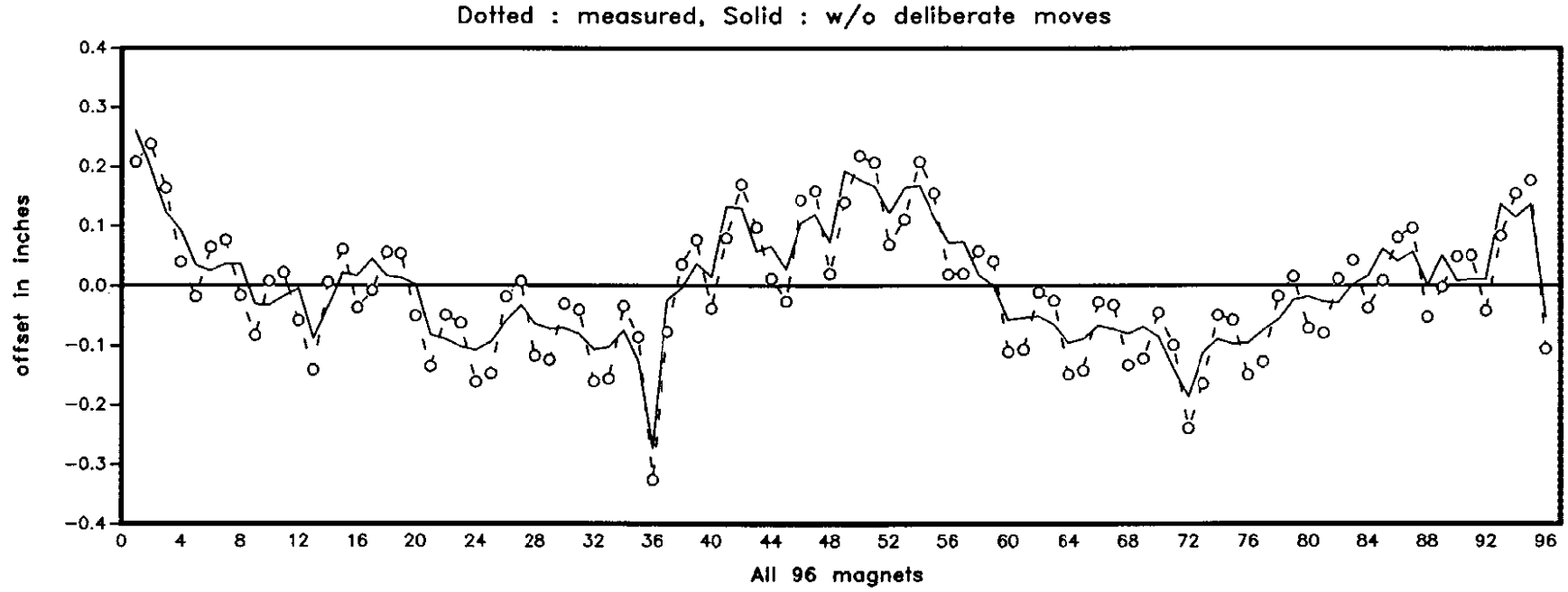

Figure 2(b): Vertical magnet offset 04/87

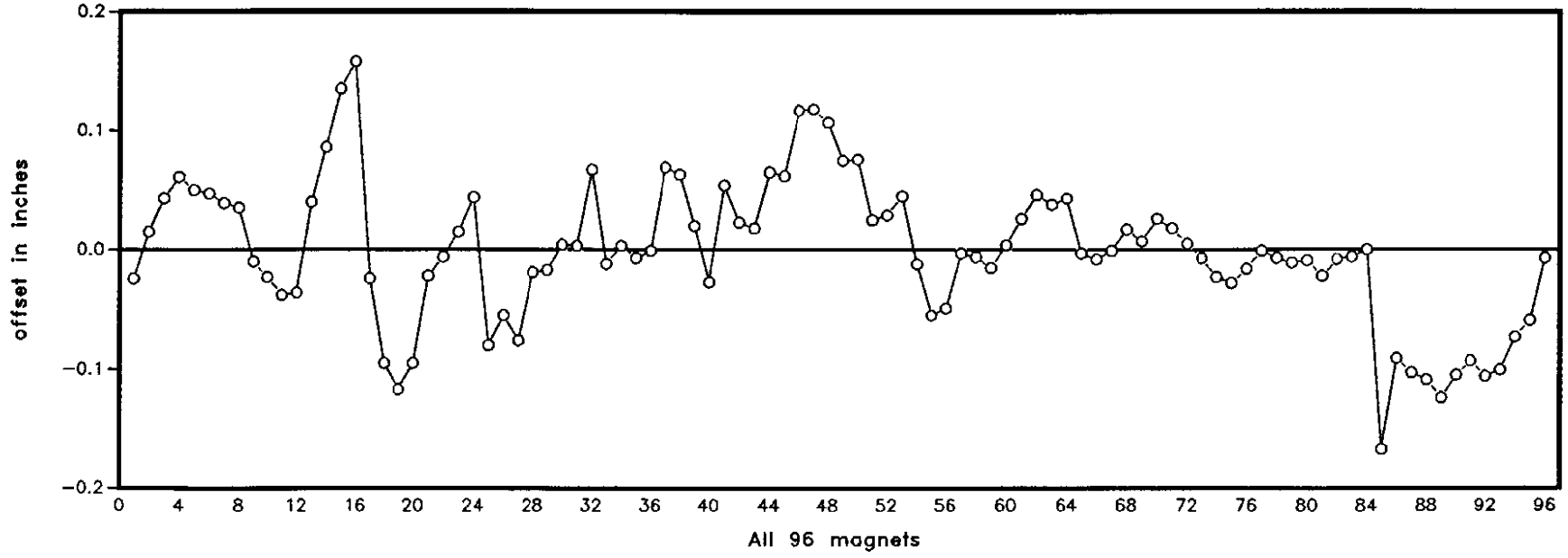

Figure 2(c): Effect of the deliberate magnet moves

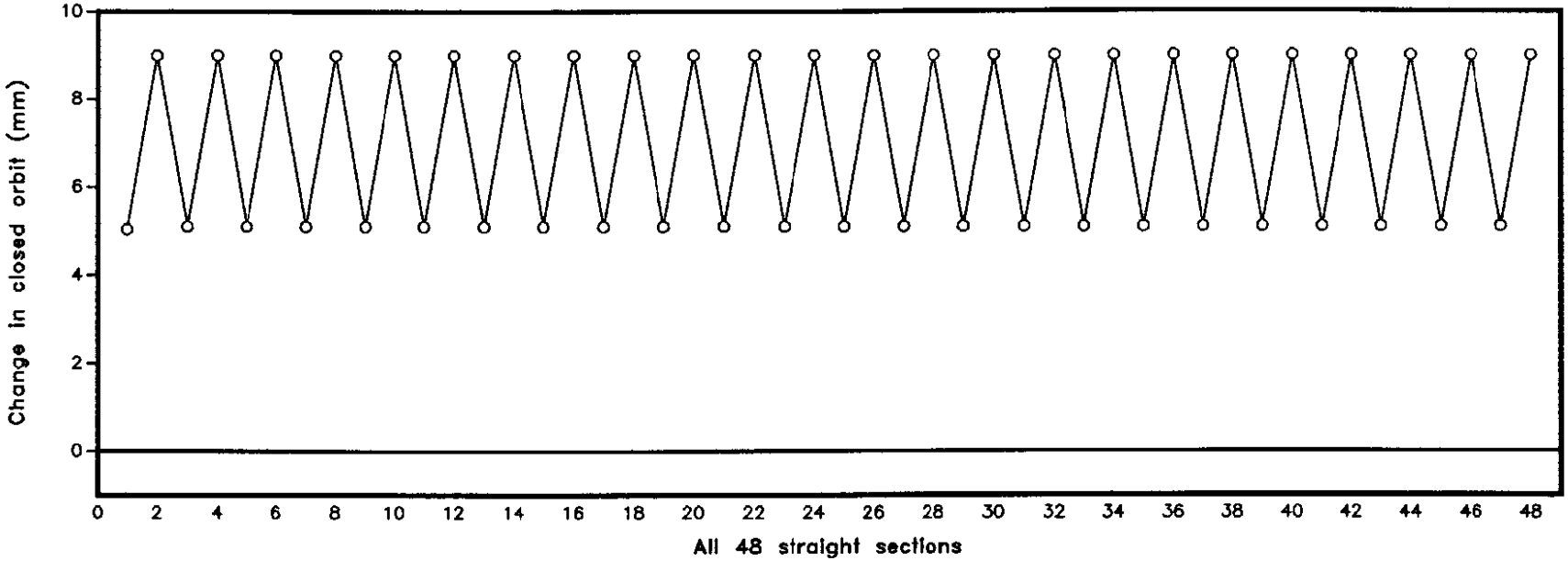

Figure 3 : Main magnet roll 04/87

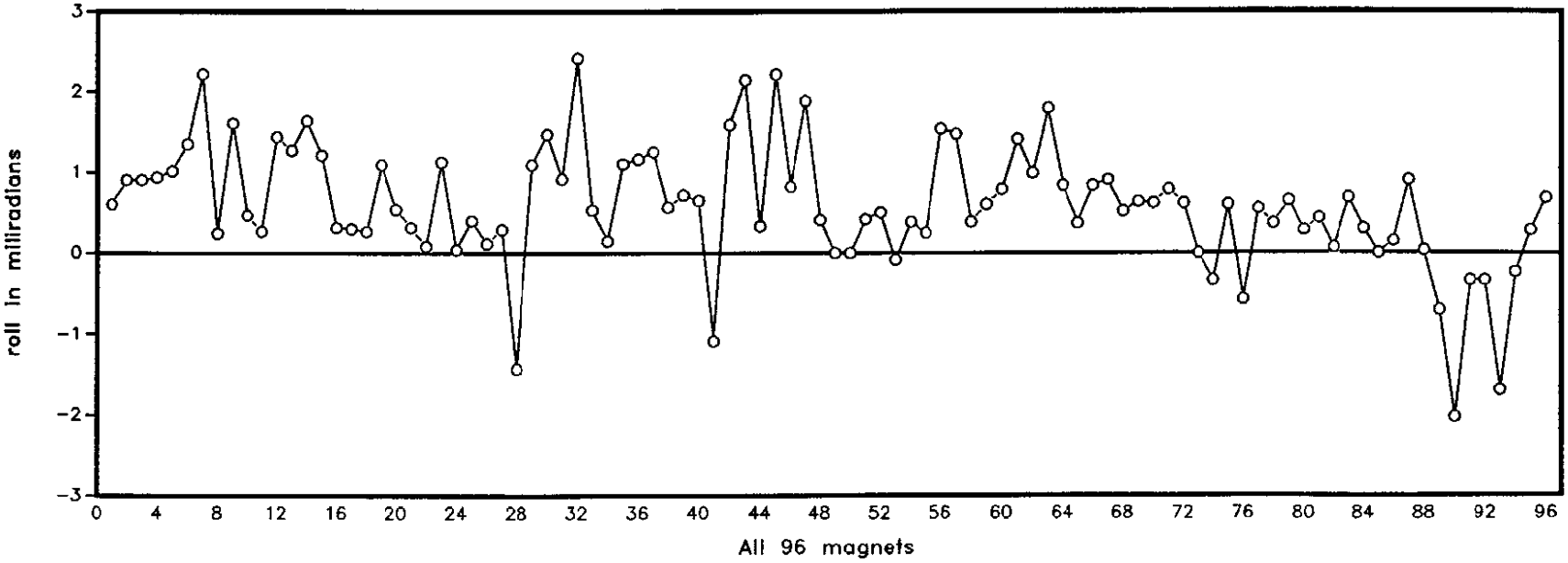

Figure 4. A typical 2-bump of 2 magnet moves

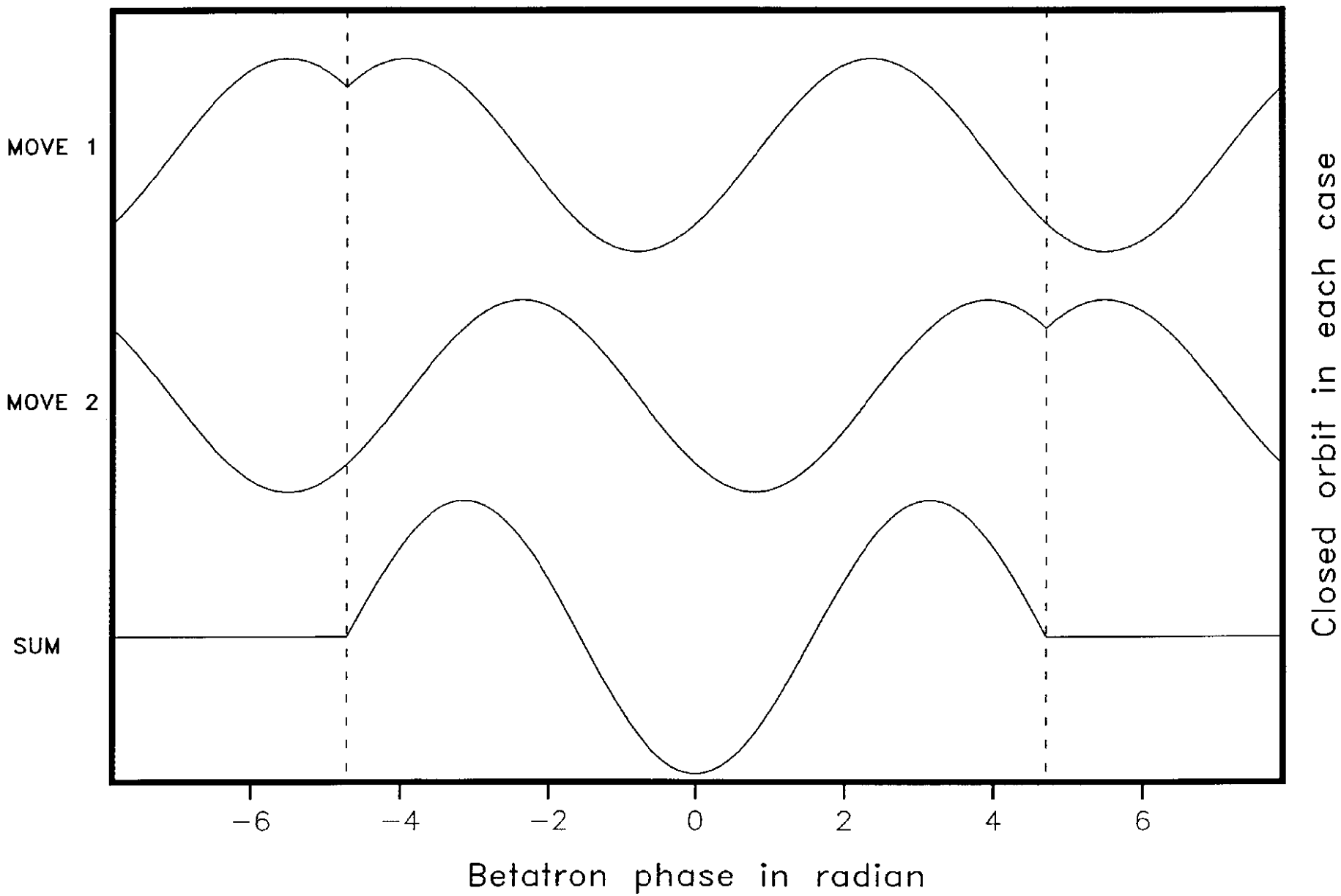

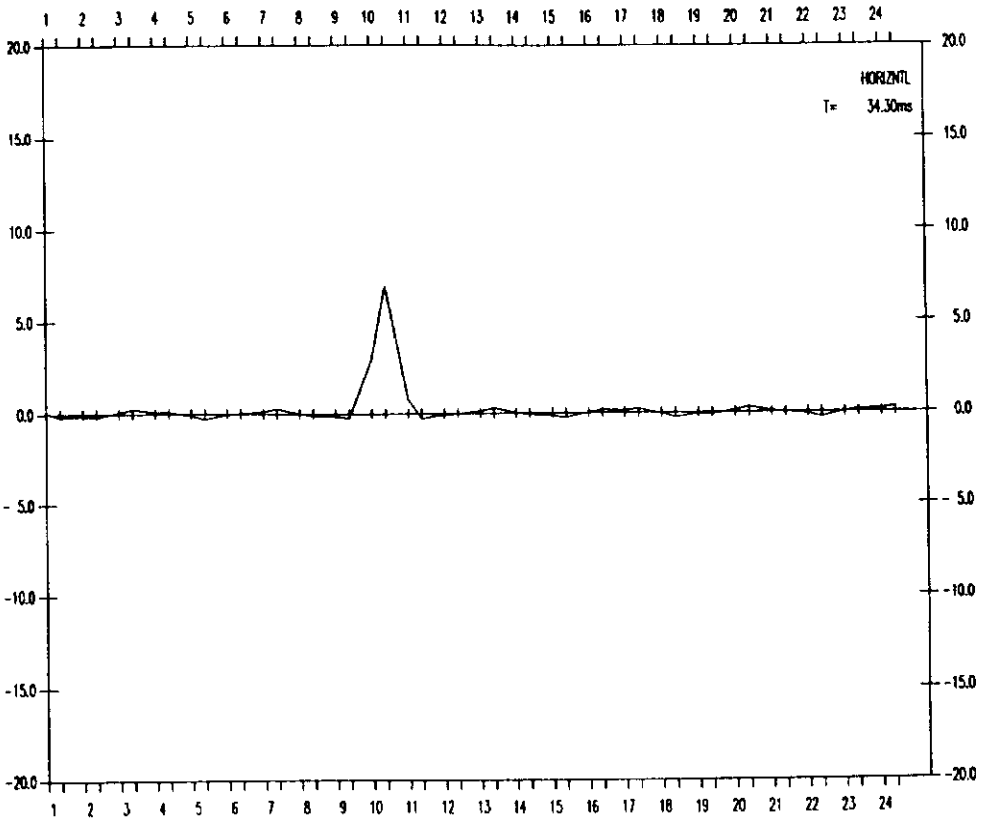

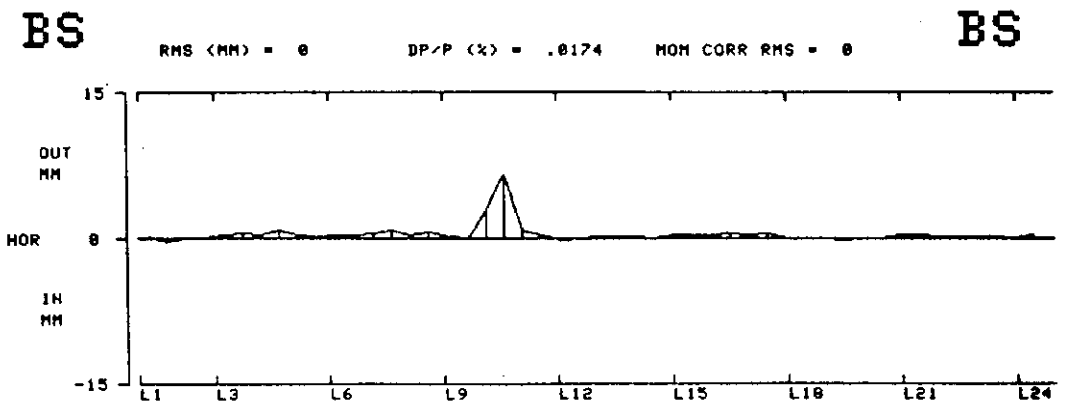

Figure 5
(a). (top) Predicted horizontal orbit change in May 1987 move
(b). (bottom) Actual horizontal orbit change in May 1987 move

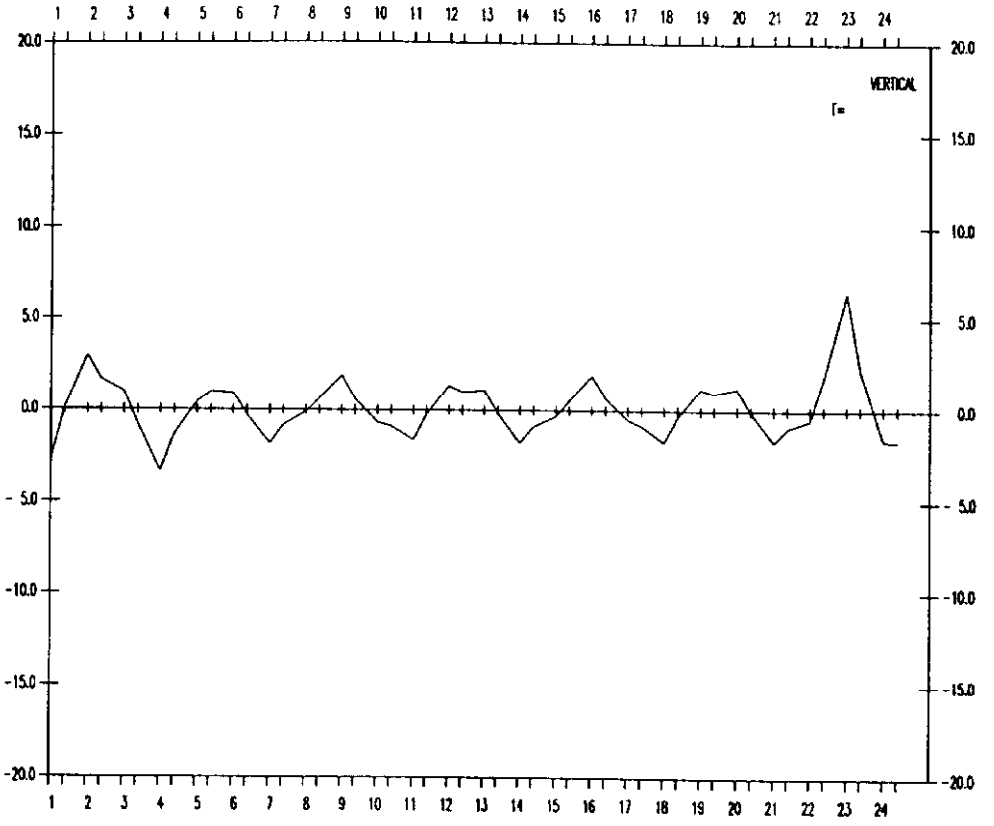

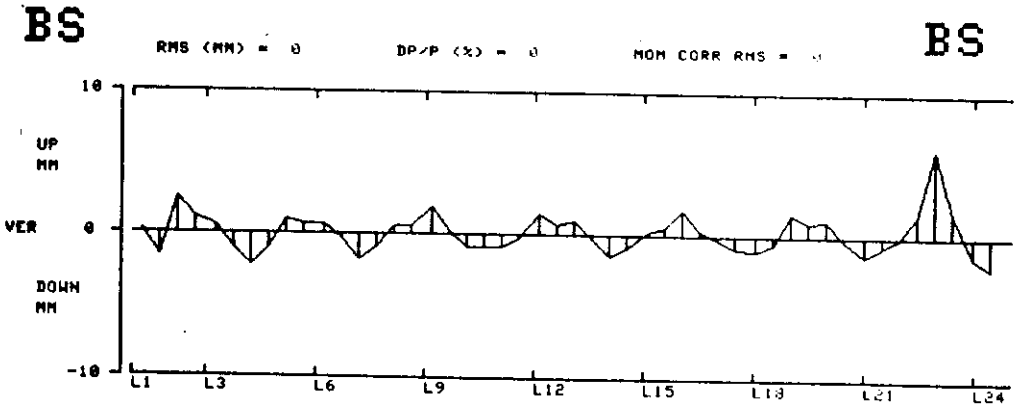

Figure 5
(c). (top) Predicted vertical orbit change in May 1987 move
(d). (bottom) Actual vertical orbit change in May 1987 move

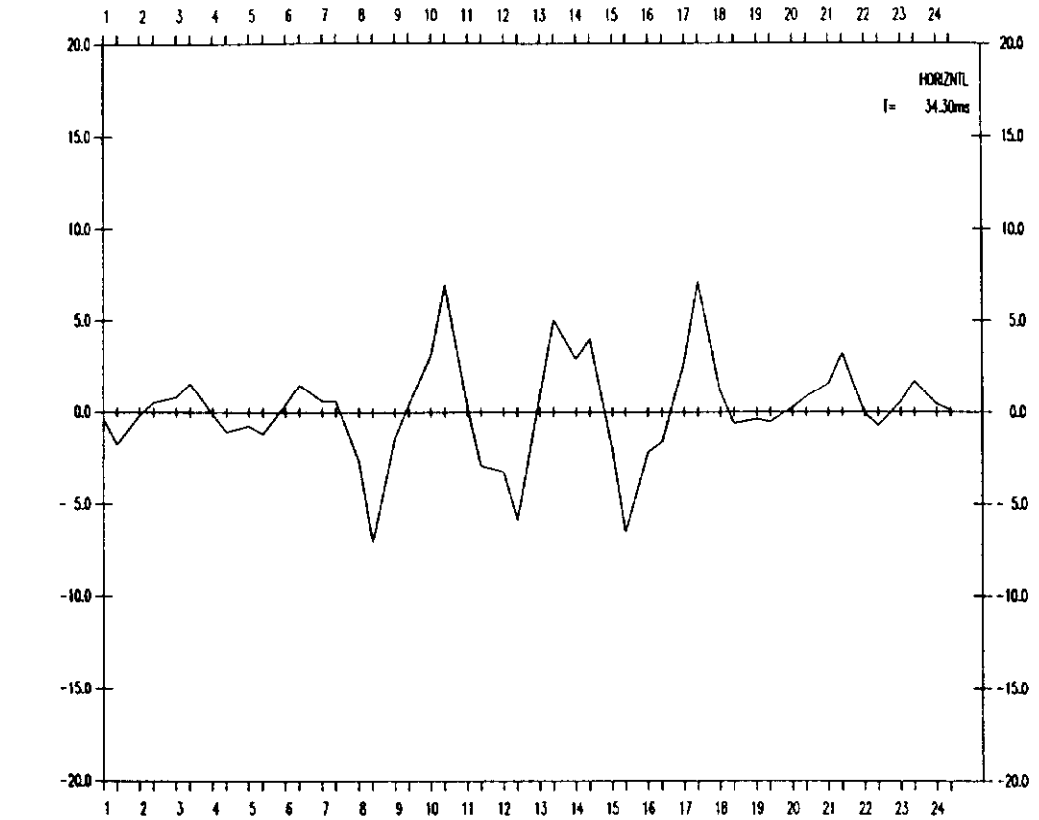

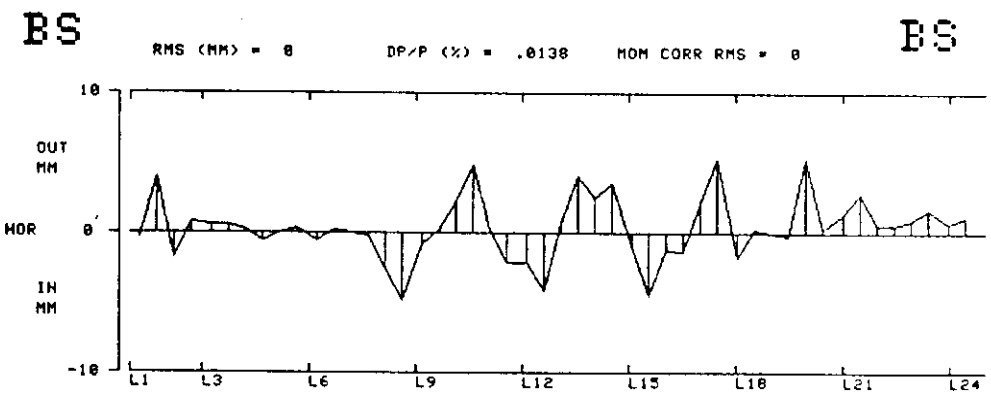

Figure 6
(a). (top) Predicted horizontal orbit change in March 1988 move
(b). (bottom) Actual horizontal orbit change in March 1988 move
(The horizontal BPM's at S1 and L20 were not functional at the time the data were taken.)

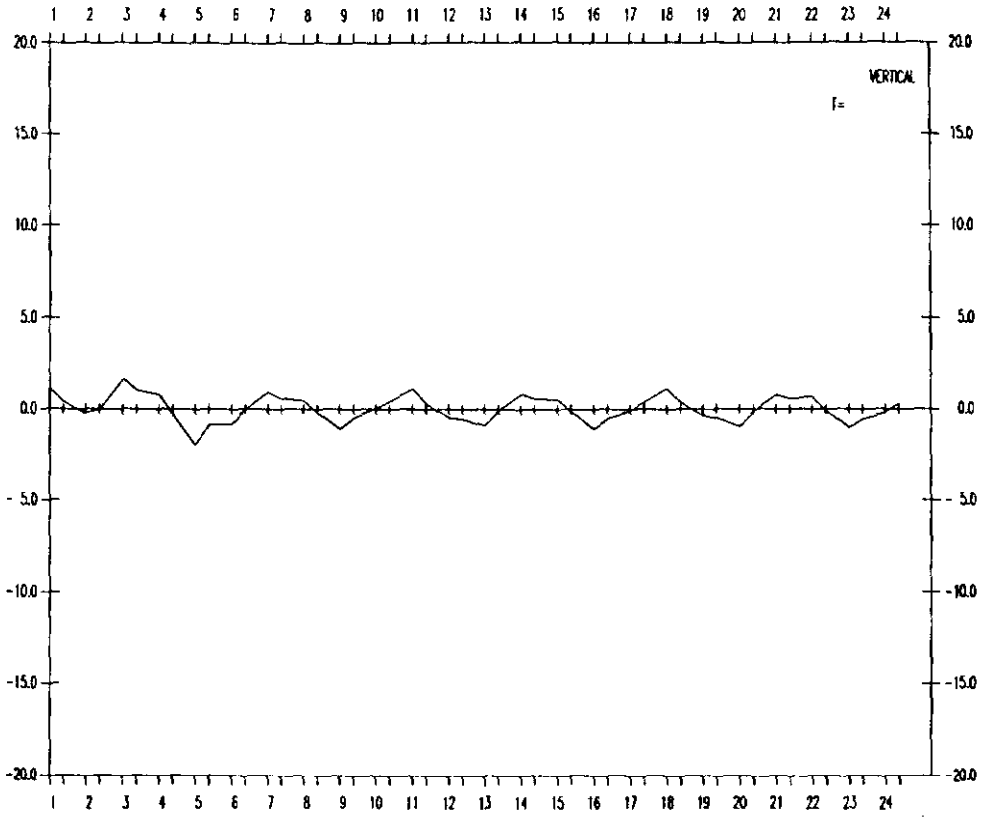

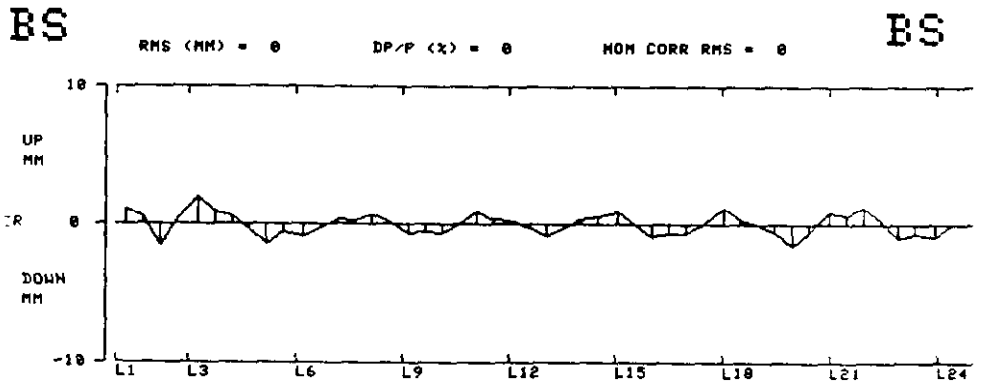

Figure 6
(c). (top) Predicted vertical orbit change in March 1988 move
(d). (bottom) Actual vertical orbit change in March 1988 move

Figure 7(a). Horizontal offsets before and after move

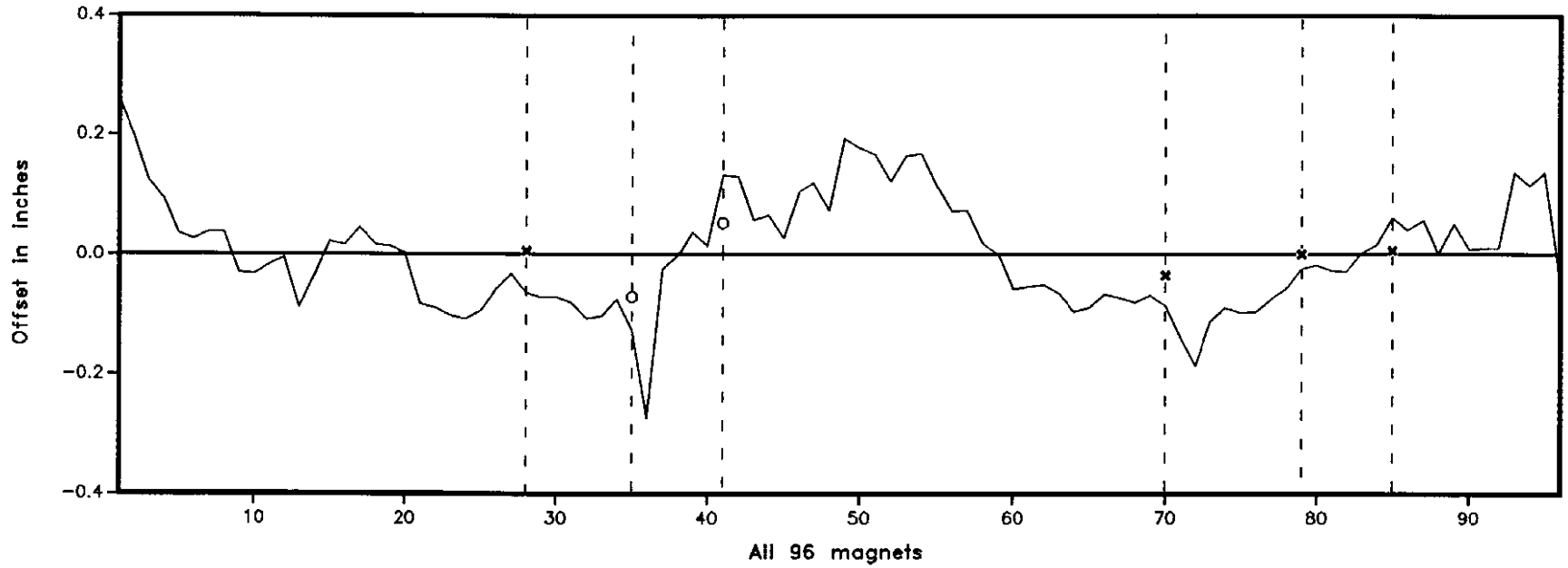

Figure 7(b). Vertical offsets before and after move

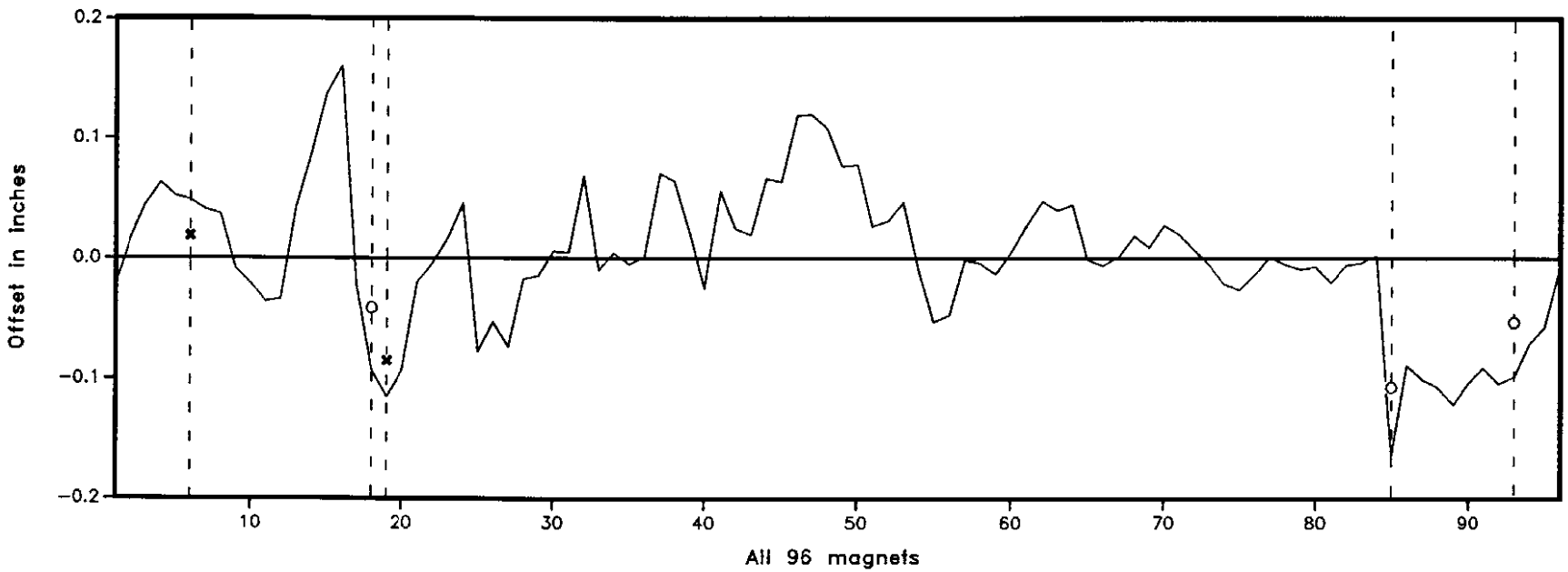

Figure 8 Horizontal orbits

solid: measured, dotted: predicted

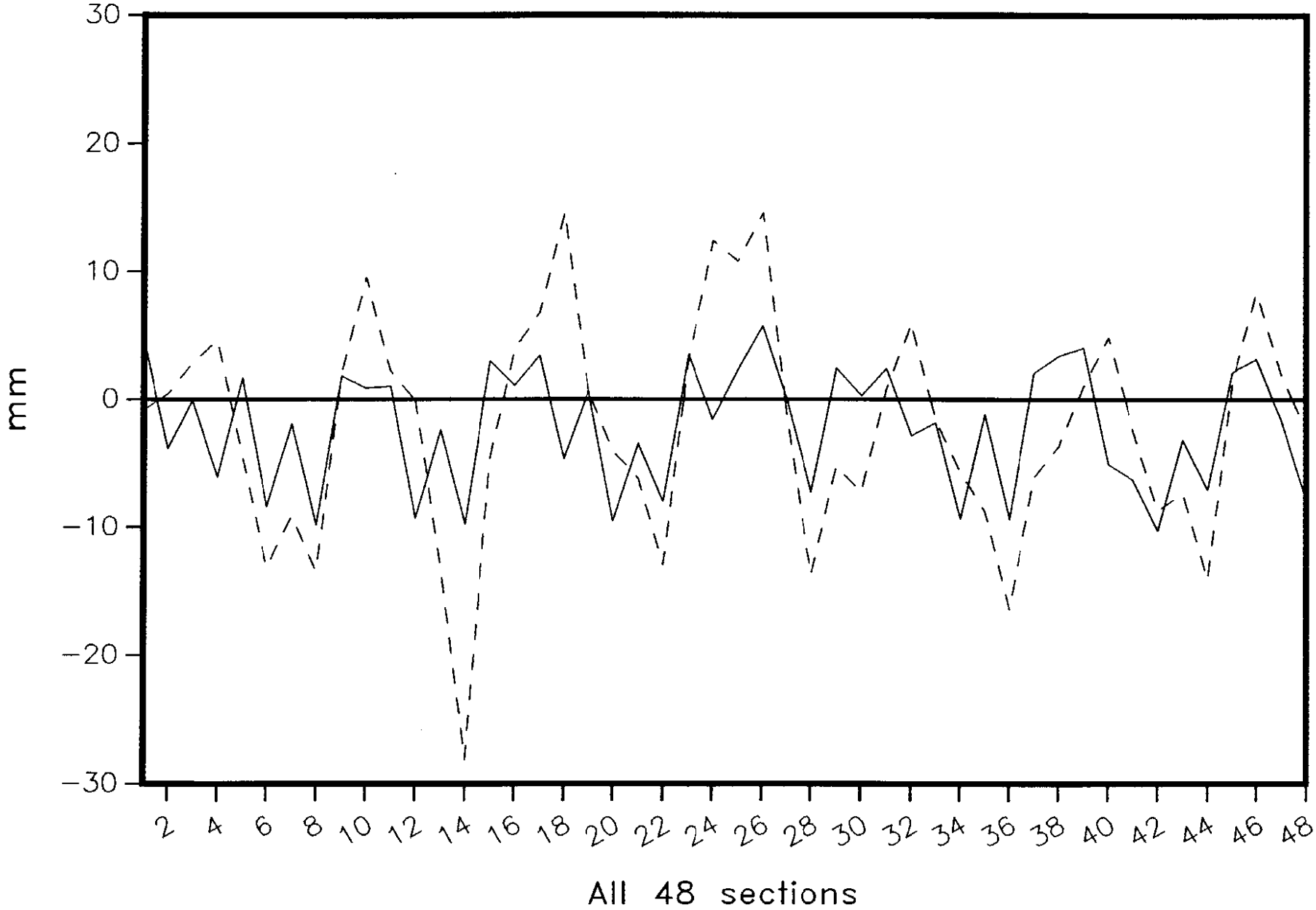

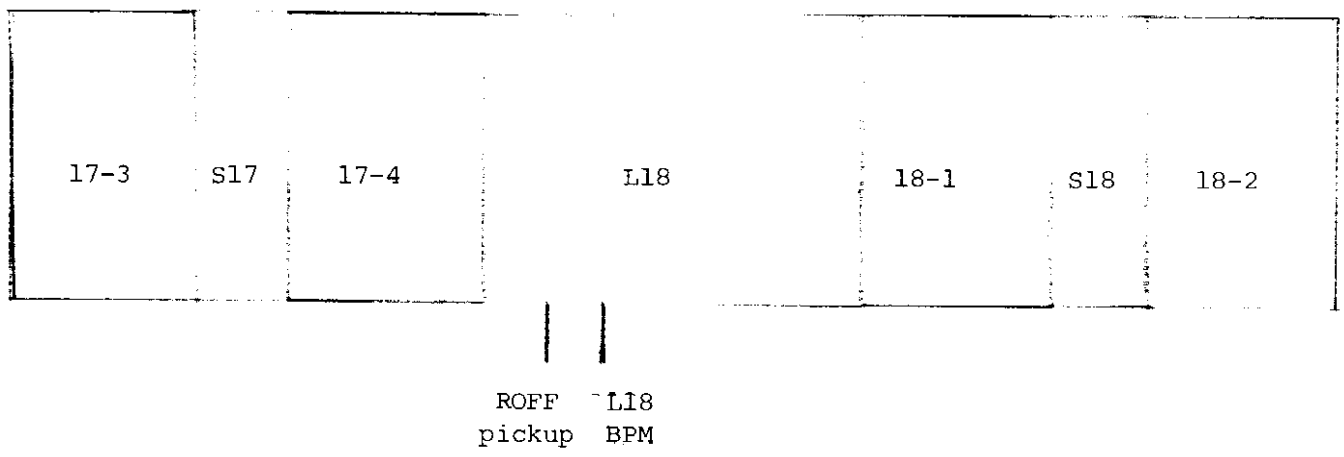

Figure 9. Layout of the vicinity of ROFF pickup

Figure 10 Vertical orbit

solid: measured, dotted: predicted

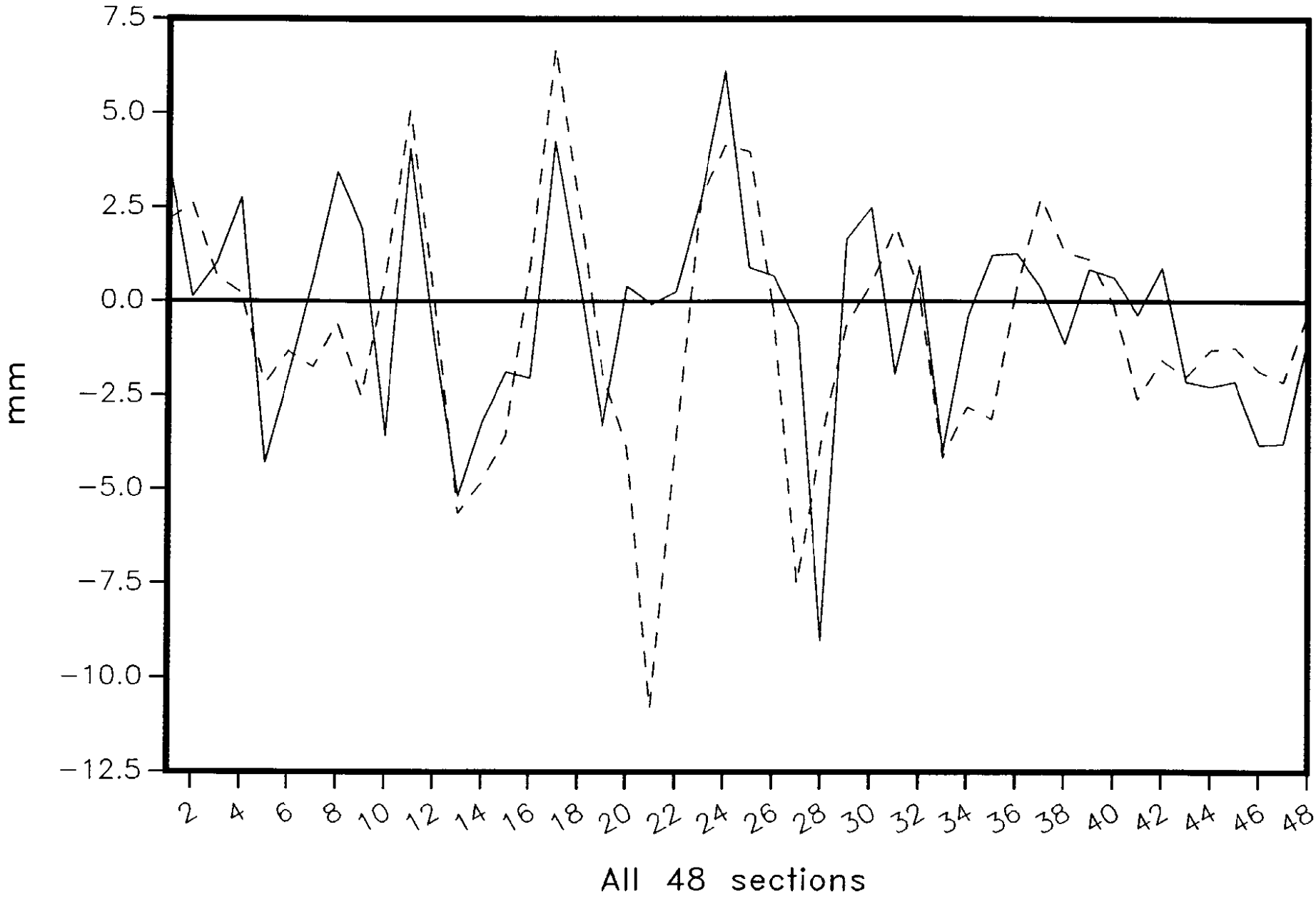

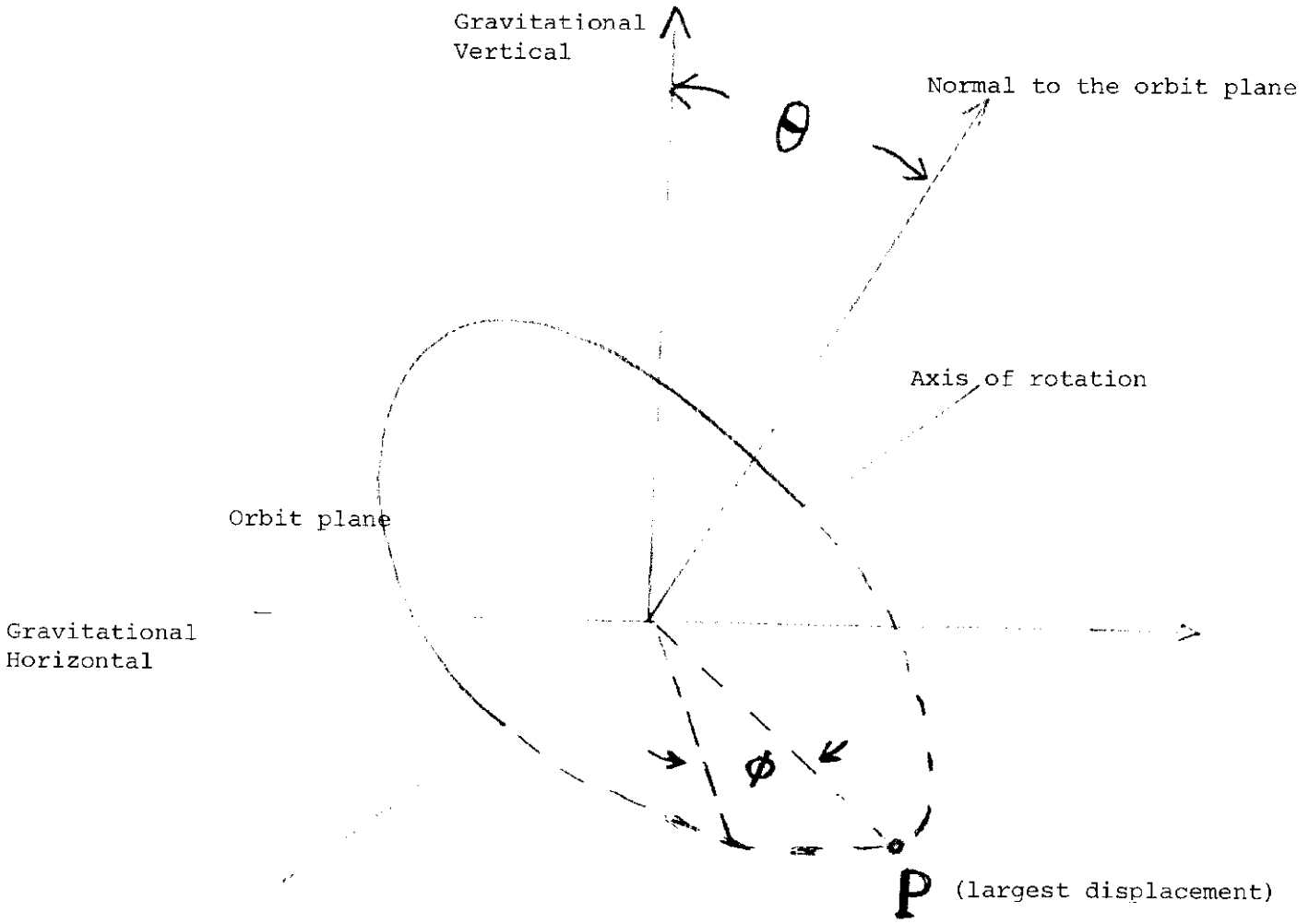

Figure 11. Geometry of the tilted orbit plane

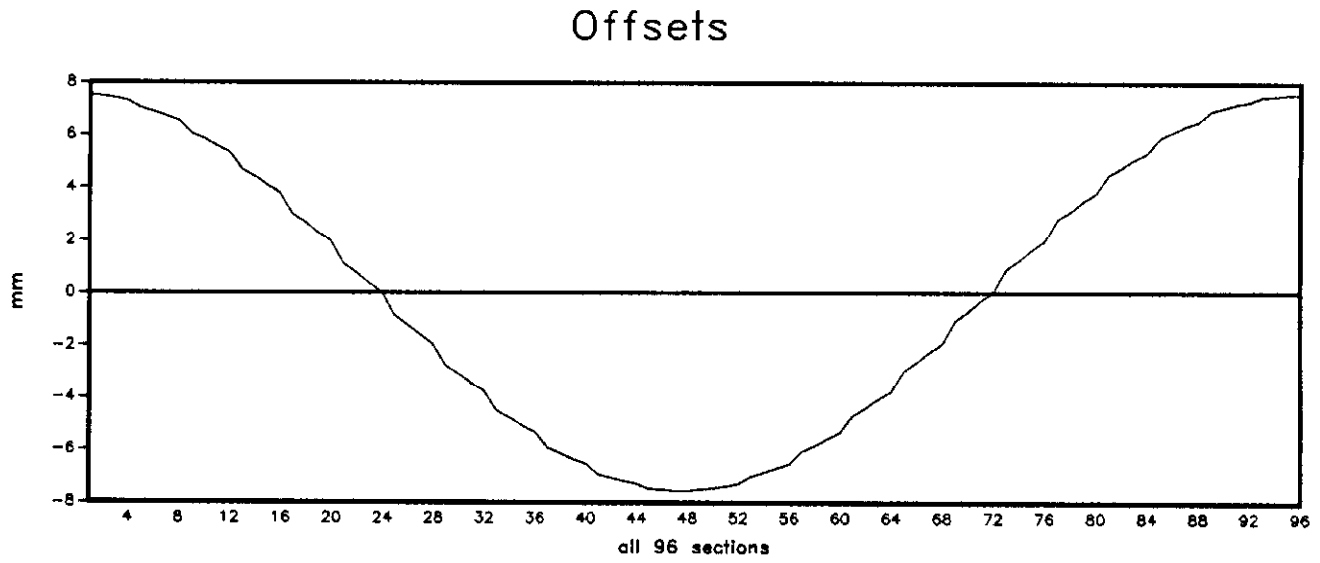

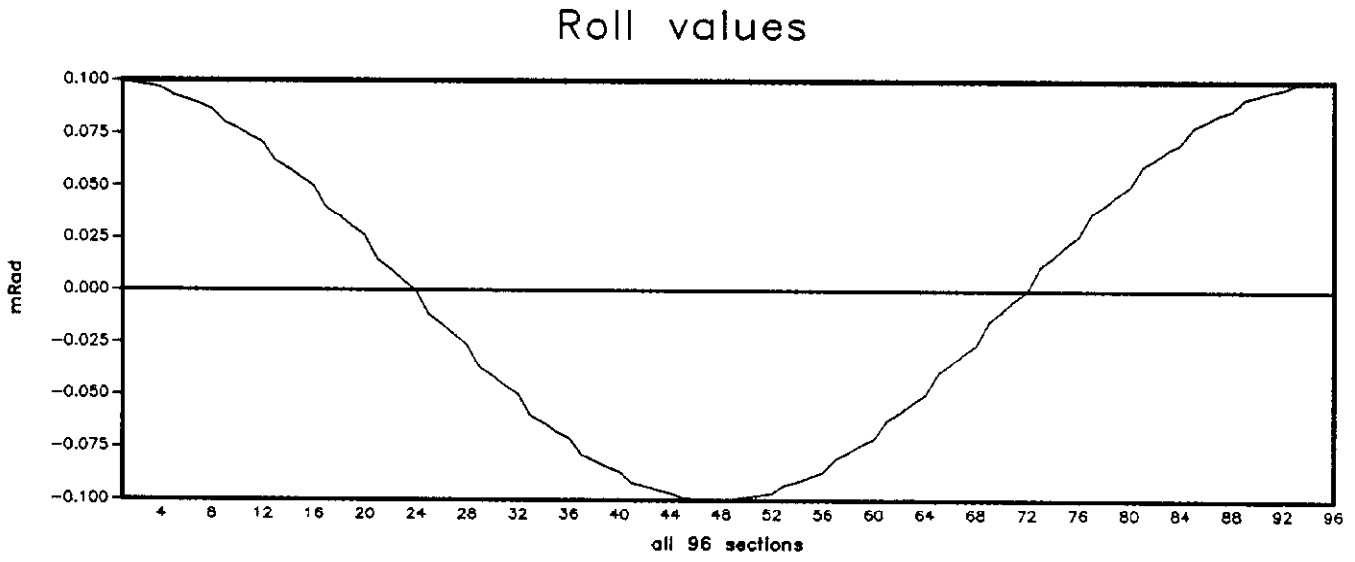

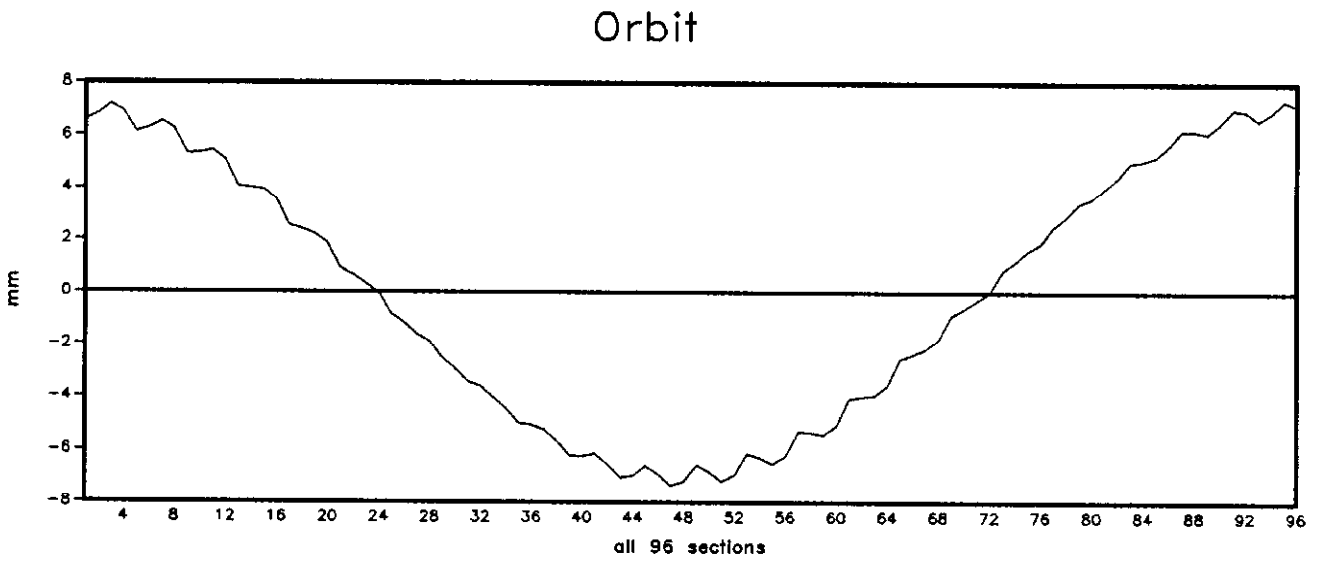

Figure 12. Effects of a tilt of 0.0001 radian